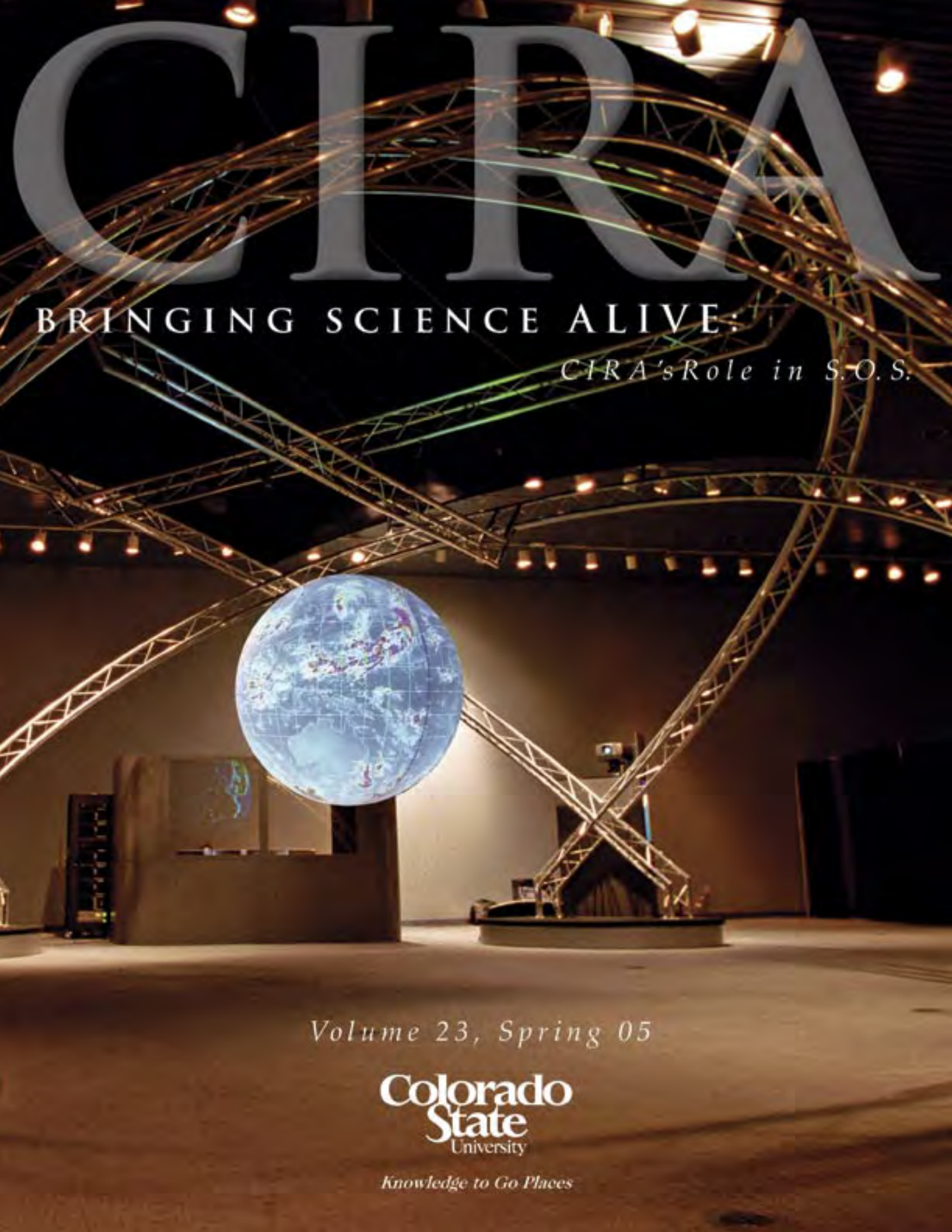


CIRA



BRINGING SCIENCE ALIVE:

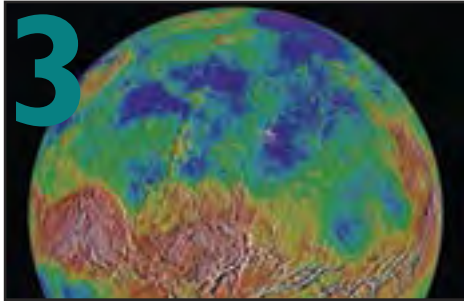
CIRA's Role in S.O.S.

Volume 23, Spring 05

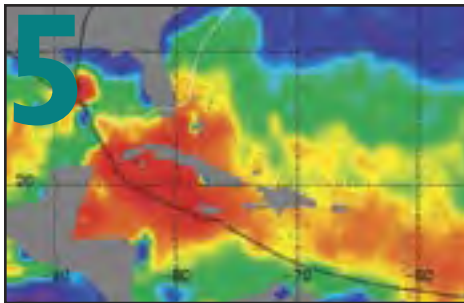
**Colorado
State**
University

Knowledge to Go Places

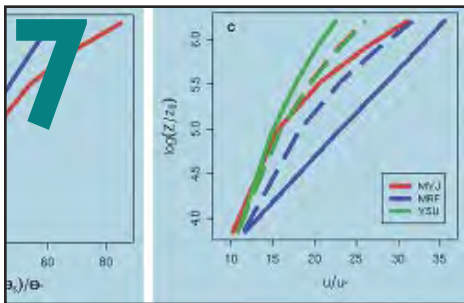
Contents



NOAA Science On a Sphere.....3



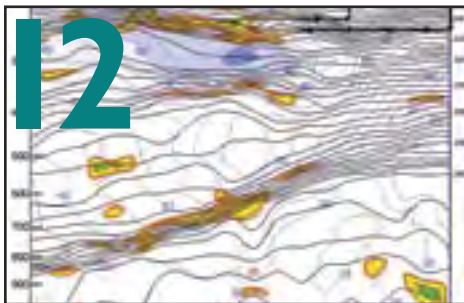
CIRA Contributions to the Joint Hurricane Testbed5



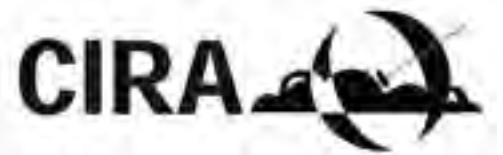
A Modeling Study on the Performance of WRF PBL Schemes7



The Visibility Information Exchange Web System – VIEWS.....9



Turbulence Generation Associated with Gravity Waves in the Vicinity of an Upper-Level Jet 12



Cooperative Institute for Research in the Atmosphere

CIRA Advisory Board

Steven R. Abt, Colorado State University
Interim Dean of Engineering
Marie C. Colton, Director, NOAA/
NESDIS/ORA
Peter K. Dorhout, Colorado State University
Interim Vice Provost for Graduate Education
Hank Gardner (Chairperson), Colorado State
University Associate Vice President
for Research
Richard D. Rosen, Assistant Administrator,
NOAA/OAR
Steven A. Rutledge, Colorado State University
Atmospheric Science Department Head
Thomas H. Vonder Haar, Director of CIRA
and University Distinguished Professor,
Colorado State University Department
of Atmospheric Science (ex officio)

CIRA Advisory Council

Hal C. Cochrane, Professor, Colorado State
Department of Economics
Mark DeMaria, Team Leader, NOAA/
NESDIS/RAMM
Mark DeMaria (Acting), Chief, NOAA/
NESDIS/ORA/ARAD
Sonia M. Kreidenweis-Dandy Professor,
Colorado State Department of Atmospheric
Science
“Sandy” E. MacDonald, Director,
Forecast Systems Laboratory
Thomas H. Vonder Haar (Chairperson)
Director of CIRA and University
Distinguished Professor, Colorado State
University Department of Atmospheric
Science

Magazine Staff Editor

Mary McInnis-Efaw, Editor
Laura Grames, Assistant Editor

Design

University Relations, Colorado State
University

Technical Committee

Bernadette Connell, Doug Fox,
Cliff Matsumoto, Donald Reinke

NOAA Science On a Sphere

By Michael Biere and Steve Albers

As we all were taught in grade school, a globe is the only accurate way to present a map of the entire earth. Global datasets just cannot be accurately represented on a flat surface. Science On a Sphere™ (SOS) updates the trusty globe, bringing it into the age of computers and global remote sensing datasets. Much as a planetarium realistically portrays the wonders of the night skies, SOS vividly and accurately portrays the wonders of our Earth, other planets and moons, even the sun. The visual impact of SOS is hard to grasp without actually seeing it in person. The size and three-dimensionality of the system are essential, and can't be represented in a photograph.

Invented (patent pending) by Dr. Alexander MacDonald, head of NOAA's Forecast Systems Laboratory (FSL), SOS is essentially a six-foot spherical movie screen with a set of computer-driven projectors shining on it. Custom software provides the magic of the theater, coordinating the projected data into a seamless animated globe. The authors are CIRA researchers among those at FSL work-

ing to further enhance and perfect the SOS software and displayed datasets.

SOS Datasets

NOAA global remote-sensing and modeling activities provide an abundant source of data for display on the sphere, only a small part of which have been incorporated into SOS at this time. Global infrared satellite imagery, sea surface temperatures, climate models, X-ray sun imagery, earth bathymetry, and surface elevation data are among the NOAA datasets we commonly display on the sphere. NASA datasets also provide a look at other planets and moons of our solar system.

As a demonstration of the versatility of displaying diverse scientific datasets on SOS, we have also been assembling global images of a number of Solar System objects. In many cases, this involves image processing to mosaic and/or combine datasets from spacecraft images

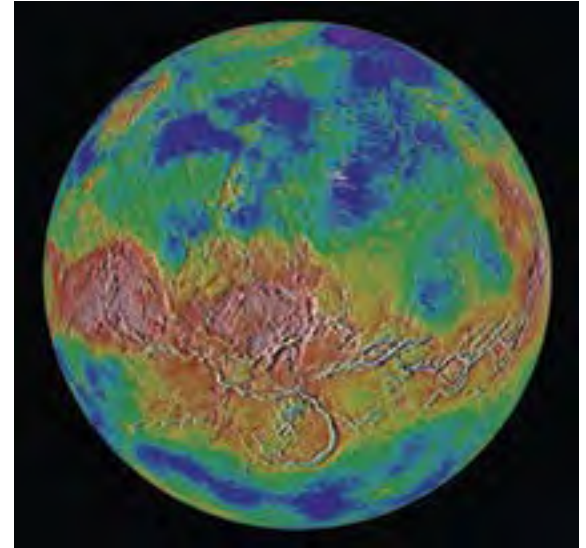


Figure 1. A shaded relief topography map of Venus was created using hue information from an image by Calvin Hamilton with intensity information from a bump map by A. Tayfun Oner. The original data is from NASA's Magellan mission.

and maps available from various sources. We show a couple of examples (Venus and Io) in Figures 1 and 2.

(continued on page 4)

Fellowships in Atmospheric Science and Related Research

The Cooperative Institute for Research in the Atmosphere at Colorado State University (CIRA) offers a limited number of one-year Associate Fellowships to research scientists including those on sabbatical leave or recent Ph.D. recipients. Those receiving the awards will pursue their own research programs, collaborate with existing programs, and participate in Institute seminars and functions. Selection is based on the likelihood of an active exchange of ideas between the Fellows, the National Oceanic and Atmospheric Administration, Colorado State University, and CIRA scientists. Salary is negotiable based on experience, qualifications, and funding support. The program is open to scientists of all countries. Submitted applications should include a curriculum vitae,

publications list, brief outline of the intended research, a statement of estimated research support needs, and names and addresses of three professional references.

CIRA is jointly sponsored by Colorado State University and the National Oceanic and Atmospheric Administration. Colorado State University is an equal opportunity employer and complies with all Federal and Colorado State laws, regulations, and executive orders regarding affirmative action requirements. In order to assist Colorado State University in meeting its affirmative action responsibilities, ethnic minorities, women and other protected class members are encouraged to apply and to so identify themselves. The office of Equal Opportunity is in Room 101, Student Services Building.

Senior scientists and qualified scientists from foreign countries are encouraged to apply and to combine the CIRA stipend with support they receive from other sources. Applications for positions which begin January 1 are accepted until the prior October 31 and should be sent via **electronic** means only to: Professor Thomas H. Vonder Haar, Director CIRA, Colorado State University, humanresources@cira.colostate.edu. Research Fellowships are available in the areas of: **Air Quality, Cloud Physics, Mesoscale Studies and Forecasting, Satellite Applications, Climate Studies, Model Evaluation, Economic and Societal Aspects of Weather and Climate.** For more information visit www.cira.colostate.edu.

NOAA Science on a Sphere *(continued from page 3)*

In addition to the examples shown here, we also worked to obtain and process a spectacular global Jupiter movie from the Cassini mission showing the cloud circulation patterns over a 10-day interval. A color map of Europa was created using a highly processed combination of two other maps, with high resolution detail from the USGS and lower resolution color information from space artist Bjorn Jonsson. The original data for the Io and Europa maps are from NASA's Voyager and Galileo missions.

We are currently working on a number of global maps for satellites of Jupiter and Saturn to be displayed on SOS. For Saturn, this involves using IDL to re-project and overlay new Cassini images on top of previously made maps based on Voyager data. Other ongoing efforts include developing a movie showing the history of population growth on the Earth, as well as improved displays of the Sun and Earth's moon.

NOAA Planet Theater

The value of SOS as an educational tool has been convincingly established at this point. The system was enthusiastically received by Broomfield Heights Middle School students in a pilot curriculum project in Broomfield, Colo. (See Figure 3.)

The use of SOS in a museum setting was demonstrated at the Maryland Science Center

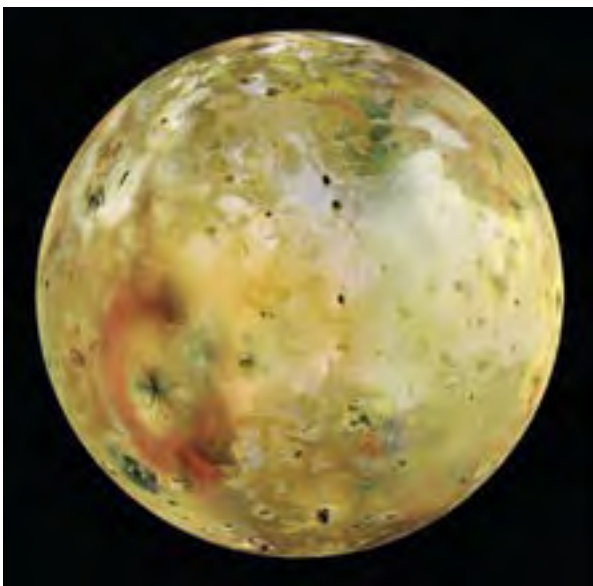


Figure 2. A color map of Jupiter's satellite Io was created by combining three Galileo mosaics and mapping them along with a base map from a Celestia software space artist.



Figure 3. Students at Broomfield Heights Middle School using SOS in a pilot curriculum (NOAA photo by Will von Dauster).

in Baltimore. A very positive detailed report evaluating the use of SOS at the museum was prepared for the Maryland Science Center by RMC Research Corporation. Quoting from their report: "Across all age groups, visitors mentioned the educational value of Science on a Sphere." They wrote in conclusion:

"Comments throughout the surveys reflected visitors' enjoyment of the experience and suggest that it was a rich and successful learning experience. Visitors described the exhibit as 'cool,' 'riveting,' 'fantastic,' 'fascinating,' 'magical,' 'phenomenal,' 'informational,' 'educational,' and as the 'best in the museum.' Visitors appreciated the Sphere as an aesthetic experience, a piece of innovative technology, and as a compelling and versatile educational tool for children and adults."

The next challenge for the SOS project is to get the system out of the lab and into museums and science centers where its educational potential can be realized. SOS project personnel envision a NOAA Planet Theater™ featuring SOS,

akin to the IMAX™ theaters and planetariums currently in such venues. Turning this dream into a reality is the big-picture driver behind our day-to-day activities.

Enhancements to SOS

We are currently designing a more compact layout for SOS with additional projectors closer to the sphere in order to decrease the footprint needed by the system. We anticipate a number of benefits from this new architecture. More projectors will increase the visual level of detail and brightness. Moving the projectors between the viewers and the sphere will avoid any shadowing of the sphere by the viewers.

Much of the audience impact from the current generation of SOS depends on experienced projectors guiding an audience through the numerous datasets that we display. To extend the utility of SOS to venues or times when such projectors are not available, we expect to add interactive capabilities to the system so that a viewer can interact with the sphere via a museum-style kiosk display. Developing narrated and interactively annotated media for the sphere should make SOS a compelling exhibit even where dedicated staff is not available for presentations.

CIRA Contributions to the Joint Hurricane Testbed

By Mark DeMaria, John Knaff, Julie Demuth, Raymond Zehr, and Jack Dostalek

Transitioning new forecasting techniques and algorithms from research to operations has been termed “Crossing the Valley of Death;” unless concerted efforts are made to ensure that new developments are tested and implemented, they can languish and never be fully realized. To facilitate this transfer for tropical cyclone applications, NOAA established the Joint Hurricane Testbed (JHT) in 2001. In this program, funding is provided on a two-year cycle for promising research applications that are ready to be tested in an operational environment at the National Hurricane Center (NHC) in Miami. At the end of the evaluation period, a decision is made by NHC whether or not to make the application operational, depending on the performance and upkeep requirements. CIRA has participated in the JHT over the past several years, and two new products were declared operational after the testing period. Two additional products currently are in the evaluation phase, with real-time testing to occur during the 2005 tropical season. This article briefly describes these four JHT projects developed by NESDIS and CIRA.

Completed JHT Projects at CIRA

The first cycle of JHT projects occurred in 2002-2003. Methods for improving intensity analysis and forecasting were deemed a very high priority by the JHT. Accordingly, CIRA received funding to test: (1) a new method for estimating tropical cyclone intensity and structure from the Advanced Microwave Sounding Unit (AMSU) and (2) a new version of the Statistical Hurricane Intensity Prediction Scheme (SHIPS) that utilizes satellite information.

The AMSU instrument first became available in 1998 on the KLM series of NOAA’s operational polar-orbiting satellites. The AMSU instrument has the advantage over infrared satellite measurements in that it can penetrate below the tops of clouds and provide information about the vertical structure of a tropical cyclone. The temperature structure near the tropical cyclone is retrieved

from the AMSU measurements, and dynamical relationships are used to estimate the wind field. Figure 1 shows an estimate of the symmetric part of the wind (averaged azimuthally at various radii from the storm center) as a function of radius and height, from the AMSU retrieval technique as applied to Hurricane Felix during the 2001 Atlantic hurricane season. Although the horizontal resolution of the AMSU instrument – which, at best, is 48 km – is not sufficient to capture the small-scale features near the storm center, the method provides a reasonably accurate estimate of the wind structure. Other parameters can be derived from AMSU data (e.g., pressure drop, temperature anomalies), and statistical methods are used to relate these parameters to the observed maximum wind and the radii of 34-, 50- and 64-kt winds, which are required by NHC. The size and intensity algorithms were developed using AMSU data from 1999-2001. After an evaluation during the 2002 and 2003 hurricane seasons, the algorithms were made operational by NHC in 2004. Further details of the AMSU algorithm can be found in Demuth et al (2004).

Hurricane intensity forecasts have considerably less skill than track forecasts. To improve the ability to forecast intensity changes, a new, experimental version of NHC’s operational Statistical Hurricane Intensity Prediction Scheme (SHIPS) was developed. In the past several years, the empirically based SHIPS model has shown greater forecast skill than more general dynamical prediction systems. The SHIPS model uses a multiple regression technique with the intensity change as the dependent variable and factors such as sea surface temperature (SST) and vertical shear of the horizontal wind in the storm environment as independent variables. However, a limitation of the SHIPS model was that it did not include much information about the storm itself due to a lack of observations. Also, the effect of the ocean was represented by the SST alone, but recent research has shown that

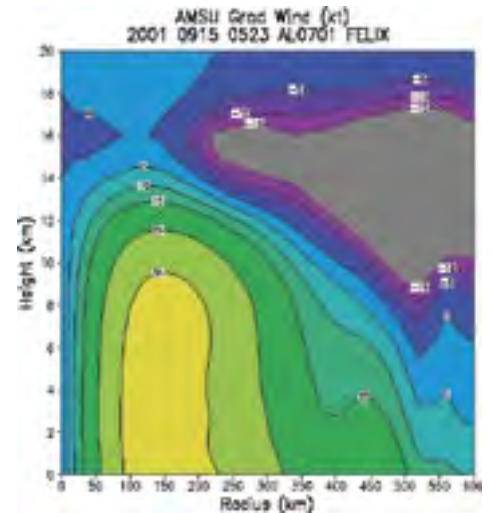


Figure 1. The AMSU-derived symmetric wind field (kt) from Hurricane Felix as a function of radius from the storm center and height. The retrieval underestimates the inner core winds, but the basic structure with cyclonic flow at low levels (positive winds) and anticyclonic flow (negative winds) at upper levels is very realistic.

the thermal structure of the ocean down to about 100 meters can affect intensity changes (e.g., Shay 2000). To improve the SHIPS model, an experimental version was developed using new predictors from satellite data, including inner core convective structure parameters determined from GOES infrared data and the ocean heat content (OHC) estimated from satellite altimetry data. The OHC analysis was developed in cooperation with NHC and the University of Miami. Figure 2 shows an example of the OHC analysis used as input for Hurricane Ivan from the 2004 season. This figure shows that there were considerable variations in the OHC along the track of this storm. Statistical analysis showed that OHC values in excess of 50 kJ/cm² favor intensification.

The experimental version of SHIPS was tested in real time during the 2002 and 2003 hurricane seasons in both the Atlantic and eastern North Pacific tropical cyclone basins, and results showed that the satellite input improved the forecasts by 3 to 7 percent.

(continued on page 6)

Joint Hurricane Testbed *(continued from page 5)*

PRE-IVAN – Upper Oceanic Heat Content

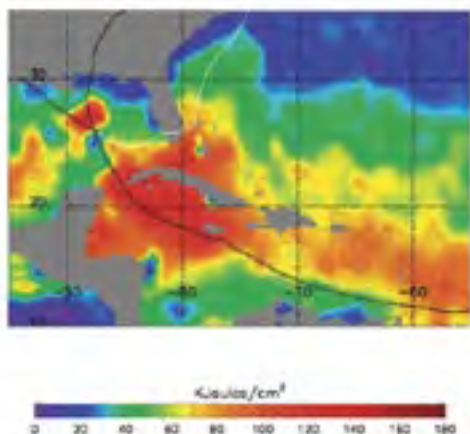


Figure 2. The ocean heat content estimated from satellite altimetry data used in the intensity forecast for Hurricane Ivan from the 2004 hurricane season. The black and white lines show the path of Ivan. After making landfall near the Florida-Alabama border, the remnants of the storm moved off the coast of North Carolina, moved south (as indicated by the white line), and became a tropical cyclone again in the Gulf of Mexico.

Based upon this success, the satellite version of SHIPS was declared operational for the 2004 season. For further evaluation, the non-satellite version was run in parallel during the 2004 season. Figure 3 shows the forecast improvement due to the satellite input in SHIPS. The satellite data improved the 2004 Atlantic forecasts by almost 4 percent and the east Pacific forecasts by more than 9 percent. This improvement represents a substantial advance in operational intensity forecasts compared to NHC's normal improvement rate of approximately 1 percent per year over the past several decades. Further details on the SHIPS model with the satellite data can be found in DeMaria et al (2005).

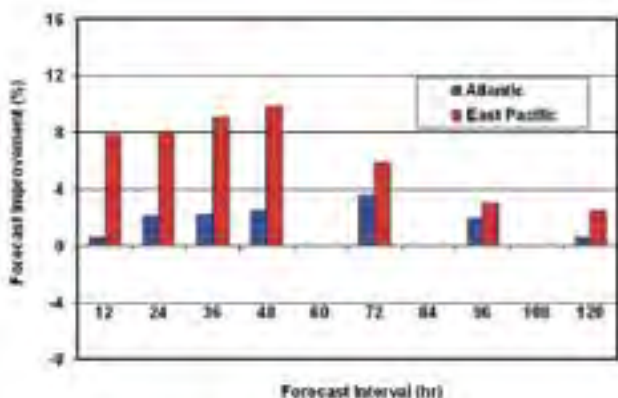


Figure 3. The improvements in the operational SHIPS forecasts during the 2004 hurricane season due to the inclusion of satellite observations.

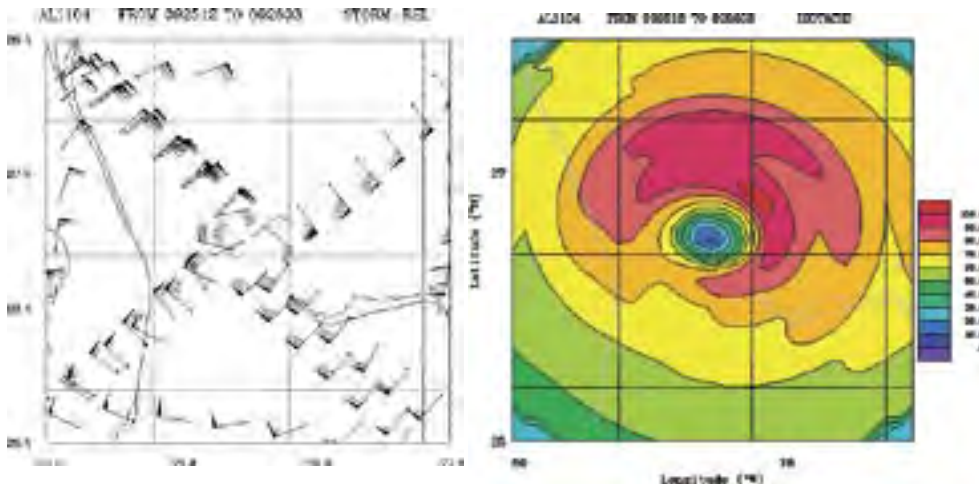


Figure 4. The flight-level winds (left) and objective analysis (right) of wind speed from Hurricane Jeanne during the 2004 Atlantic hurricane season.

Current JHT Projects at CIRA

New tropical cyclone algorithms are being developed and tested as part of ongoing JHT projects at CIRA. The ability to further improve the SHIPS model through the incorporation of aircraft observations and horizontal structure information from GOES satellites is being investigated. Although the aircraft reconnaissance data are available only in a limited part of the Atlantic basin, they usually are collected for the storms that have the greatest potential to affect the U.S. To utilize these data in a fully automated mode required for real-time operations, a detailed quality control and objective analysis system was developed. Figure 4 shows an example of the aircraft flight-level winds and the objectively analyzed wind speed field that will be utilized by the SHIPS intensity model.

Parameters from the wind field such as those shown in Figure 4 are being tested for the ability to predict intensity changes. The aircraft winds are being combined with radial structure information from GOES infrared imagery. In the previous JHT project, the satellite information was included in the SHIPS model in a fairly simple way (i.e., area averages of brightness temperatures and the corresponding standard deviations). In the current proj-

ect, more sophisticated pattern recognition techniques are being applied to extract the maximum information from the imagery. The new version of SHIPS with the aircraft input and IR pattern recognition method will be tested during the 2005 hurricane season.

Although the ability to forecast tropical cyclone tracks and intensity is improving, there will always be forecast errors. To help quantify the uncertainty, a probability model is also being developed as part of the JHT. A Monte Carlo method is being applied, which accounts for uncertainties in the track, intensity, and wind-structure forecasts from NHC. In this method, the performance of the NHC forecasts from the past several years is used to generate the appropriate probability distributions. The output of the model is the probability of 34-, 50-, or 64-kt winds during the five days covered by the official NHC forecast. The Monte Carlo model was tested in real time during the 2004 hurricane season. A version was also developed for the western North Pacific for use by the Joint Typhoon Warning Center in Honolulu. Figure 5 shows an example of the probability estimate for 34-kt winds from 15 September 2004 when there were two tropical cyclones in the Atlantic and one off the coast of Mexico. A number of new operational products are under development at NHC that will utilize the Monte Carlo model.

(continued on page 7)

Conclusions

Although the transition of forecasting methods from the research to the operational environment is sometimes called “Crossing the Valley of Death,” several algorithms and new forecast methods developed at NESDIS and CIRA are now operational at the National Hurricane Center. NOAA’s Joint Hurricane Testbed has helped to make this transition possible.

References

Demuth, J.L., M. DeMaria, J.A. Knaff, and T.H. Vonder Haar, 2004: Evaluation of Advanced Microwave Sounder Unit tropical cyclone intensity and size estimation algorithms. *J. Appl. Meteor.*, **43**, 282-296.

DeMaria, M., M. Mainelli, L.K. Shay, J.A. Knaff, and J. Kaplan, 2005: Further Improvements to the Statistical Hurricane Intensity Prediction Scheme (SHIPS). *Weather and Forecasting*, in press.

Shay, L.K., G.J. Goni, P.G. Black, 2000: Effects of a warm oceanic feature on Hurricane Opal. *Mon. Wea. Rev.*, **128**, 1366-1378.

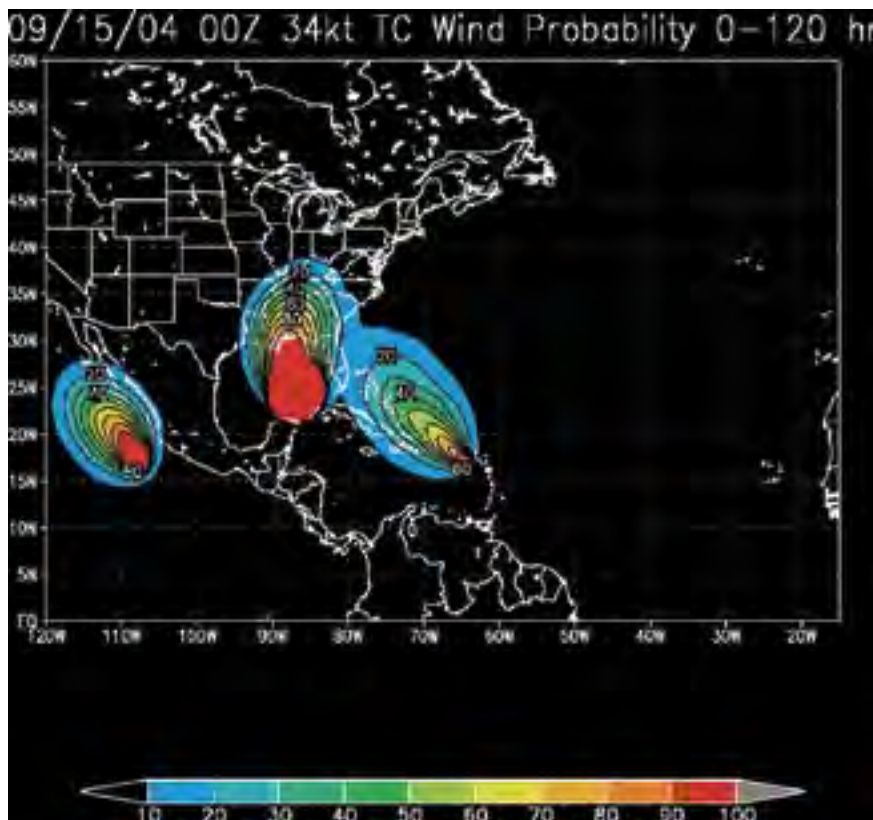


Figure 5. An example of the output from the Monte Carlo probability model. The plot shows the probability of 34-kt winds for the 5-day period beginning at 1200 UTC on 15 September 2004. There were three tropical cyclones in the model domain at this time.

A Modeling Study on the Performance of WRF PBL Schemes

By Mariusz Pagowski

The Monin-Obukhov similarity theory and results from LES provide a framework for determining vertical profiles of wind, temperature, and humidity in the surface and mixed layer. The purpose of this study is to assess how boundary layer parameterizations employed in WRF compare with theory and LES. Here, only results for a convective surface layer are presented. For complete results the reader is referred to publication in *Preprints of the WRF Users' Workshop* in June 2004.

A one-dimensional model was developed to study the behavior of the following PBL schemes implemented in the WRF model: Mellor-Yamada-Janjic (MYJ), MRF, and

YSU. A simple sinusoidal-in-time surface temperature forcing was prescribed. Several model levels were placed in the surface layer (SL) so that the results of the model could be compared with the Monin-Obukhov similarity. For simplicity, only the dry results are presented.

In Figures 1a, b, and c, profiles of potential temperature and wind from the similarity and from the three PBL schemes for different stability conditions are presented. It can be noted that the MYJ scheme fails to sufficiently transfer heat between the surface and the atmosphere, since the temperature difference between the atmosphere and the surface is several times larger than the cor-

responding value prescribed by the similarity. In both the MRF and YSU schemes, heat transfer between the surface and the atmosphere is also underestimated but not as significantly as for the MYJ scheme. The MRF temperature profile seems to be lacking proper curvature in the SL as the scheme mixes the air above too strongly. Referring to the results for the different stability regimes, in the neutral conditions, all of the schemes quite accurately follow logarithmic wind profiles prescribed by the similarity. In stable conditions, potential temperature profiles suggest that in the MYJ scheme, the gradient between the atmosphere and the surface is too steep compared to the similarity, as was

(continued on page 15)

CIRA Communiqué: Employee News

Employment Milestones

CIRA is proud to report that the following 10 employees are marking significant milestones in their tenure with Colorado State University. Celebrating 10 years with CSU are **Rodger Ames, Bernadette Connell, and Alfred Frisch. Steve Albers, Louie Grasso, John Knaff, Jim Ramer, Tracy Smith, and Julie Winchester** are all marking 15 years. Finally, **Dr. Vonder Haar** makes the list this year with 35 years of service. Congratulations to them all!

GLOBE

CIRA/CSU has been involved with the GLOBE program since its beginning in 1995. To date, more than 25,000 teachers from 107 countries have participated in GLOBE workshops and students have reported just over 11 million GLOBE measurements. This past fall, GLOBE received a prestigious \$25,000 Goldman Sachs Foundation Prize for Excellence in International Education. GLOBE was among more than 400 applicants, and the program was recognized in the Media and Technology category. The Goldman Sachs Foundation is a global philanthropic organization funded by The Goldman Sachs Group, Inc. The mission of the foundation is to promote excellence and innovation in education and to improve the academic performance and lifelong productivity of young people worldwide. In accord with that mission, GLOBE is now sponsoring a field campaign called GLOBE ONE, involving students and scientists investigating the impacts of farming practices in Black Hawk County, Iowa. GLOBE engages students during the critical years (grades 5 and 6) when many of them drop out of the math and science pipeline.

DOC Technology Transfer Award

In the truest spirit of CIRA's cooperative agreement with NOAA, CIRA researchers have an integral role in the work being done at the federal lab in Boulder. We have just learned that the federal researchers supporting the Range Standardization and Augmentation (RSA) project were nominated for a DOC Technology Transfer Award. RSA is a

project aimed at providing high resolution analyses and forecasts to support space center activities at Cape Canaveral and Vandenberg AFB, utilizing LAPS and the MM5 mesomodel. Unfortunately, CIRA Research Associate **Steve Albers** was not eligible to be nominated since he is not a federal employee. However, Forecast Systems Lab Chief John McGinley made clear that Steve's key contributions to RSA were part of the reason this nomination was possible.

AP Star Award



Dr. Cliff Matsumoto

Dr. Cliff Matsumoto, CIRA's Associate Director, was recently honored with an AP (Administrative Professional) Star Award. Cliff was recognized for his work on behalf of APs

not only at CIRA, but throughout the University as a former member of the AP Council and most recently as an important member of the University Benefits Committee. Cliff's efforts have been noteworthy and include his important role in creating the AP Research Associate/Research Scientist ladder. CIRA is proud that one of our leaders has been recognized as among the finest by his peers. Congratulations, Cliff!

Kevin Micke was also honored with an AP Star Award. Kevin came to work at CIRA to provide computer support in a part-time capacity in May of 2002 and was hired full time in March of 2004. From the beginning Kevin has been a consistently reliable and



Kevin Micke

valuable member of the team. He responds promptly when problems arise, multi-tasks with no apparent stress, and solves most problems with little or no fuss. He generally knows what to do to keep the CIRA machines working properly, and when he doesn't have the answer, he is always able to find it quickly. His attitude is unfailingly positive, upbeat, and supportive, so his nomination by his peers in the RAMM Team was well-deserved. Congratulations to Kevin!

Recent Promotions at CIRA

CIRA management was pleased to recognize the outstanding accomplishments of six individuals with special promotions as of February 1. These promotions are a part of the career ladder recently implemented by Colorado State University for Administrative Professionals. Congratulations to the following folks: **Laura Grames** to Research Associate II; **Tom Kent** to Research Associate III; **Mike Leon** to Research Associate II; **Sean Madine** to Research Associate IV; **Manajit Sengupta** to Research Scientist II; and **Jebb Stewart** to Research Associate II.

2004 Best Web Tool Award



Kevin Brundage

Kevin Brundage was recognized with the 2004 FSL "Best Web Tool" award for his Product Inventory Generator (PIG) script program written in python for the RUC Web page

to generate common products and tables with links for the eight different versions of the RUC and WRF models.

The Visibility Information Exchange Web System – VIEWS

By Rodger Ames, Doug Fox, Shawn McClure, Tom Moore, Bret Schichtel

The Visibility Information Exchange Web System (VIEWS) is an online system designed to acquire, manage, and provide access to data and metadata related to visibility and air quality, specifically to support the efforts of five Regional Planning Organizations (RPOs) in meeting the requirements of the Environmental Protection Agency's Regional Haze Rule. The Rule requires states and tribes to develop and implement plans to reduce the pollution that causes visibility impairment in 156 National Parks and Wilderness areas designated by the Clean Air Act as Class I areas, to achieve natural visibility conditions (no manmade visibility impairment) by 2064.

The primary purpose of VIEWS is to aid RPOs in the analysis and interpretation of air quality data so they in turn can provide technical support to the states and tribes. The IMPROVE dataset has regulatory significance under the Regional Haze Rule, and VIEWS provides access to custom IMPROVE data products. VIEWS makes these and a variety of supporting datasets available via a web-based interface that includes ad hoc query and custom display tools. Supporting aerosol datasets from other sponsoring agencies include FRM, STN, CASTNet, and a variety of other aerosol, optical, and meteorological data. Examples of how the IMPROVE and supporting datasets can be used to better understand visibility reduction in protected areas are shown using VIEWS analysis tools. Available tools include descriptive charting capabilities, back trajectory analysis, and a GIS-based metadata browser. We will briefly describe the fully developed database behind VIEWS which is customized to provide web access to air quality data and facilitate the import and quality control of new datasets.

Regional Planning Organizations

Five multi-state regional planning organizations are working to develop the technical basis and analyze control strategies for Regional Haze Rule (RHR)-mandated State Implementation Plans (SIP). Tribes also

have the option to prepare regional haze TIPs. Because the pollutants that lead to regional haze can originate from sources located across broad geographic areas, EPA has encouraged the states and tribes across the U.S. to address visibility impairment from a regional perspective.

Funded by the EPA, the five regional planning organizations are tasked to: a) develop and evaluate technical information to help understand how their states' and tribes' pollution sources impact Class I areas, and; b) develop regional strategies to reduce emissions of particulate matter and other pollutants leading to regional haze.

The Western Regional Air Partnership, WRAP

VIEWS is designed and funded to support all of the regional planning organizations but it had its start as an activity of the WRAP. The WRAP is a voluntary organization of Western states, tribes, and federal agencies. The Partnership promotes, supports, and monitors the implementation of recommendations from the Grand Canyon Visibility Transport Commission which was a Governor's level group created by the 1990 Clean Air Act to consider air quality and visibility throughout the West. The WRAP is conducting a regional planning process to improve visibility in all 116 WRAP region Class I areas by providing technical and policy tools needed by states and tribes. The WRAP is



Figure 1. VIEWS homepage.

administered jointly by the Western Governors' Association (WGA) and the National Tribal Environmental Council (NTEC). The WRAP recognizes that residents have the most to gain from improved visibility and that many solutions are best implemented at the local, state, tribal, or regional level with public participation.

The WRAP is made up of 14 Western states, numerous tribes, and federal agencies. The WRAP region includes the states of Alaska, Arizona, California, Colorado, Idaho, Montana, Nevada, New Mexico, North Dakota, Oregon, South Dakota, Utah, Washington, and Wyoming. Over 400 federally-recognized tribes and Alaska native villages within the WRAP region are equal partners in the regional haze planning process. Participation is encouraged throughout the Western states and tribes. Federal participants are the Department of the Interior (National Park Service and Fish & Wildlife Service), the Department of Agriculture (Forest Service), and the Environmental Protection Agency.

(continued on page 10)

The Visibility Information Exchange Web System *(continued from page 9)*

WRAP committees and forums seek consensus among the governmental partners and stakeholders including large and small businesses, academia, environmental groups, and other public interest representatives. Scientific findings and policy options are presented to policy makers and the public for appropriate discussion and response. The WRAP is committed to bringing together all those who may contribute to or be affected by poor air quality. Findings and policy options go before the WRAP Board. Tom Moore, a Western Governors' Association employee, is the technical coordinator of the WRAP and is housed at CIRA in Fort Collins. VIEWS benefits from close association with Tom and through Tom with the other RPOs.

IEWS Capabilities

The VIEWS homepage, <http://vista.cira.colostate.edu/views>, is shown in Figure 1. Links to individual RPO websites are on the right-hand side of the homepage. Below the VIEWS logo are quick links to data resources and information, such as user's guides, news and bulletins, and a current dataset inventory. The left-hand navigation bar provides links to the main website sections. Descriptions of the content and capabilities of the main VIEWS sections are presented following the top-down organization of the left-hand navigation bar.

Data and Metadata

The data and metadata section provides access to the integrated air quality datasets and related metadata in VIEWS. These resources are available via links from the *All Data* section or via the interactive *Metadata* and *Query Wizard* tools.

The *Metadata Browser* is an interactive graphical browser that displays monitoring site locations and land features in a web-based Geographical Information System (GIS). This tool provides a map with zoom and pan capabilities, high-resolution geographical layers and provides tabular metadata for single or multiple monitoring sites. The Metadata Browser incorporates the *active layer* concept common to GIS applications in which the user can select monitoring sites from an active geographical layer. For example, if the active *Counties* layer is selected, clicking on the map within a given county will select metadata for all sites in

that county. Unique to VIEWS is the ability to select a Class I area and display metadata for the representative IMPROVE monitoring sites, even if that site is not physically within the Class I area boundaries. In its tabular output, the Metadata Browser provides links to the *Site Browser* tool. The Site Browser contains detailed monitoring site metadata, links to topographic maps, and photographs.

The *Query Wizard* tool allows users to retrieve data by selecting a subset of monitoring sites, measured parameters, and time ranges from the VIEWS integrated database. Users are provided options to download data and metadata from multiple monitoring programs and select from a variety of output formats, including text files and charts.

The *ASCII Data* page provides links to a variety of files containing raw IMPROVE aerosol data and associated metadata. These data are provided in simple text format to allow easy access to relevant information. Data from all monitoring programs in VIEWS is not yet available as text files. However we are planning to add additional datasets to the file inventory. Among these will be datasets in the integrated database as well as datasets available only from the text file inventory.

The *Data Repository* page is a recent addition. This page provides descriptions and links to datasets located on the VIEWS ftp site (<ftp://vista.cira.colostate.edu/Public/DataRepository/>). It provides a location where special data, such as data from a field campaign, can be made available to the public. These datasets have been submitted by a variety of organizations and have not yet been examined by the VIEWS data management team.

Annual Summary

The *Annual Summary* section of VIEWS provides access to data products in support of states' requirements to comply with the Regional Haze Rule. These data products include graphical summaries based on IMPROVE aerosol data. The *Annual Summary* data products are updated on a yearly basis as each complete year of IMPROVE data becomes available. Calculated visibility metrics which cater to the Regional Haze Rule include the annual and 5-year mean of the best and worst 20 percent visibility

days expressed as deciview. Other parameters available from the Annual Summary are annual and seasonal means and a host of measured and calculated parameters based on IMPROVE aerosol data.

The *Annual Summary* data products are available via a series of graphical interfaces. These interactive web pages display visualizations of aerosol spatial patterns, composition information for specific data aggregations, trend lines of annual and multi-year time periods, and back-trajectories to indicate air mass source regions during specific days and haze events.

The VIEWS development team is in the process of updating the look, feel, and product content of the Annual Summary.

Resources

VIEWS hosts an extensive collection of online data resource links related to air quality, meteorology, and emissions. These resources are selected for their relevance to the study of visibility issues and for their usefulness in understanding the nature, causes, and reduction of regional haze.

The *CAPITA tools* page delivers, in cooperation with the Center for Air Pollution Impact and Trend Analysis (CAPITA) at Washington University, St. Louis, access to several unique air quality-related web services. These include state-of-the-science tools to provide the ability to virtually browse, accumulate and analyze a wide variety of data, including ground-based measurements and imagery from a variety of satellite data sets.

The *RHR Planning Docs* page has recently been added. The Regional Haze Rule requires each state (optional for tribes) to adopt emissions reductions beginning in 2008 to achieve reasonable, steady progress to improve visibility on the worst monitored days, and prevent degradation of the best monitored visibility days, at each of the mandatory Federal Class I areas. This page will serve as a clearinghouse to reflect analysis and evaluation of the IMPROVE monitoring data for planning purposes. Key analyses yet to be completed for planning purposes include: 1) the nominal increment of visibility improvement needed at each Class I area

(continued on page 11)

The Visibility Information Exchange Web System *(continued from page 10)*

by 2018; 2) relating the controllable fraction of fire and dust emissions to monitoring data; and 3) consideration of the fraction of natural visibility conditions represented in the baseline monitoring data from each Class I area.

Imagery

VIEWS hosts a series of photographs, courtesy of the IMPROVE network, documenting the spectrum of visibility conditions at many of the Class I areas. Links to webcam resources that demonstrate regional haze conditions and visibility impairment episodes are also provided. These images are selected for their relevance to the study of visibility issues and for their usefulness in providing visual motivation for the reduction of regional haze.

Development

The VIEWS *Development* section provides web tools and data products currently under development. When new tools and data products are initially developed they will be placed in the development section for initial review by the VIEWS community.

A tool currently in the development section is the *Data Browser*. The concept behind the data browser is to provide a simple, fast, and intuitive means to graphically look at any combination of data in the VIEWS integrated database. The current incarnation of the Data Browser combines geographical and charting components in a single display, with custom chart and data aggregation options.

The *Data Browser* provides a set of case studies where data across monitoring networks can be readily compared. One time series case study selects particle organic and elemental carbon data from both the IMPROVE and the Speciated Trend Network (STN) at the Puget Sound monitoring location near Seattle, Wash. Figure 2 is a map detail from the VIEWS Data Browser showing the Seattle urban area and the outlying Alpine Lakes Class I area. In Figure 2, IMPROVE monitoring locations are shown as blue dots (including the IMPROVE Puget Sound site and the Snoqualmie Pass site which is representative of the Alpine Lakes Class I area) and STN sites (scattered throughout the Seattle urban area) are shown as red dots. The STN collocated with the IMPROVE Puget Sound site is obscured

by the IMPROVE site icon. Figure 3 is a timeline of monthly average organic and elemental carbon aerosol concentrations from the IMPROVE Puget Sound monitoring site and the collocated STN monitor. Note the similarity between carbon fractions measured by the respective monitoring programs. The ability to browse and perform ad hoc data inter-comparisons using web-based graphical tools is a unique feature of VIEWS and provides a useful tool for both air quality scientists and policy analysts.

A second developmental tool is what we are terming the new Database Query Tool. This is a very powerful access tool that allows one to query the VIEWS integrated database and retrieve data in a variety of output formats. One can select particular sites, parameters, and date ranges, as well as various attributes for each data point returned. One can also make a variety of choices regarding the appearance of the data reports. This tool provides complete access to the entire integrated database.

Conclusion

VIEWS offers a variety of data products designed for use by states in satisfying their requirement to comply with the Regional Haze Rule. The data and products on VIEWS are available to RPOs, states, tribes, and all members of the general public who have an interest in issues pertaining to air quality in general and regional haze in specific that impacts National Parks, Wilderness areas, and other scenic areas in the United States.



Figure 2. Map view from VIEWS web-based GIS showing the Seattle, Wash., urban area and the neighboring Alpine Lakes Class I (Wilderness) Areas. Blue dots indicate two IMPROVE monitoring locations, and red dots urban STN sites. The STN site collocated with the IMPROVE Puget Sound site is obscured by the IMPROVE site icon.

VIEWS recognizes the need to continually augment and modify its data products.

One of the more exciting developments in the works is a multimedia visibility and air quality educational section. This section will introduce a visitor to the issues and science related to the study of regional haze in a fun, interactive tool.

One measure of a successful website is the amount of visitor traffic it receives. To date, the VIEWS website is averaging about 500 unique visitors per month from more than 90 different countries. In addition, over 50 other websites have links directing their visitors to the VIEWS website. VIEWS web-based tools and database capabilities continue to evolve in response to feedback from VIEWS users and stakeholders. The VIEWS development team is always open to

comments, suggestions, and feedback to make VIEWS responsive to the needs of its supporting air quality community.

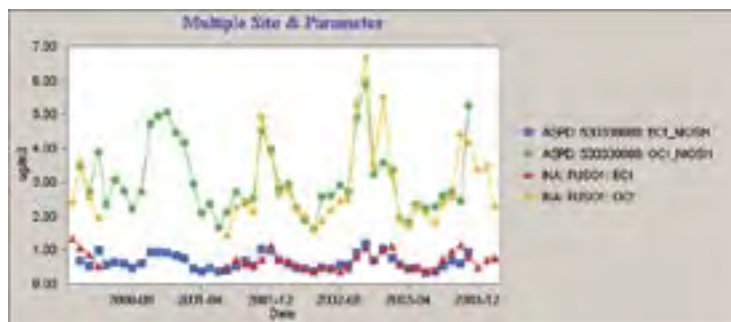


Figure 3. Time lines of monthly average fine particle organic carbon (OCf) and elemental carbon (ECf) concentrations from IMPROVE (INA) and STN (ASPD) site closest to the IMPROVE Puget Sound monitoring site. The dark blue and red markers represent EC and the green and yellow markers represent OC, from the respective monitoring programs.

Turbulence Generation Associated with Gravity Waves in the Vicinity of an Upper-level Jet

By Chungu Lu

Atmosphere/weather conditions accounted for 22.7 percent of the total cause of general aviation (excluding commuter airlines) accidents for 1999 (National Transportation Safety Board, 2003). Clear-air turbulence (CAT) is one of the most dangerous categories of atmospheric conditions for aviation safety. Understanding how CAT is generated in the seemingly quiet upper atmosphere, and predicting its occurrence, has been a scientific endeavor for many decades.

The Severe Clear Air Turbulence Colliding with Aircraft Traffic (SCATCAT) experiment was conducted as part of the Winter Storms Reconnaissance Program on 17-18 February 2001. The experiment was aimed at improving the understanding of turbulence generation mechanisms at the upper troposphere and lower stratosphere, where commercial aircraft are routinely routed. During the SCATCAT experiment, the NOAA G-IV aircraft executed a stack of four constant-altitude flights, at 10.1-, 10.7-, 11.4-, and 12.5-km levels, over the north-central Pacific Ocean. Figure 1 shows schematically these flight tracks (black-arrowed lines, with yellow segments indicating the locations where turbulence were observed), overlapped with the isentropic surface (black curves) cross-section. The isentropic surfaces and wind isotachs (blue contours, with shaded region for wind in excess of 80 m) were reconstructed from dropsonde measurements conducted during the flights. This shaded wind-maximum region displays an upper-level jet streak. The SCATCAT flights were conducted right above this jet core region, but on the northeast side of it (also refer to Figure 2 in Lu, et al 2005a). Gravity waves are apparent along the flight tracks on the top of the jet stream. The Diagnostic Turbulence Kinetic Energy Function (DTF) is calculated and plotted as contours, shaded with colors of orange, yellow, and green. Clearly, the DTF turbulence diagnostic presents large values aligned with frontal zones and at regions with substantial wind shears, but misses regions

of turbulence in association with gravity-wave activities experienced along the flight tracks.

In addition to the dropsonde measurements, many in-flight observations of meteorological and geophysical variables, such as horizontal and vertical velocity field, temperature, and Ozone concentration, etc., were carried out during the SCATCAT flight mission. These in-flight observations were sampled at a frequency of 25 Hz (a horizontal spatial scale of 9.2 m with a constant aircraft speed of 230 m), so that the fluctuations on the small scales of gravity waves and geo-fluid turbulence could be adequately resolved. The detailed information about the SCATCAT experiment is also summarized in Koch, et al (2005).

Time-frequency Analysis of Gravity Waves and Turbulence

Because of the highly non-stationary and intermittent nature of turbulence, the traditional spectral analysis cannot consistently capture the turbulence signal in a time series. The wavelet technique, on the other hand, is ideal for localizing a physical phenomenon in both spectral and physical spaces. Here we use a continuous wavelet analysis to analyze the in-flight observations. The Morlet mother function is used for the transformational kernel, which is a nearly orthogonal wave function modulated by a Gaussian window. Figure 2 is the wavelet time-frequency analysis of vertical acceleration data observed by NOAA G-IV. Two types of signals can be distinctively identified from this analysis (Fig. 2a): the slow signal (10^{-2} - 10^{-1} Hz, corresponding to spatial scales of a few tens of kilometers to a few kilometers) and the fast signal (10^{-1} - 10 Hz, corresponding to spatial scales of a few hundreds of meters to a few tens of meters). The fast signals showed less

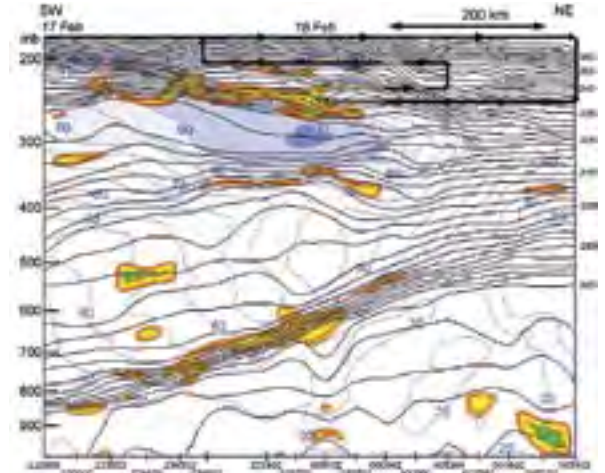


Figure 1: The four stacked legs of the G-IV tracks (at 10.1-, 10.7-, 11.4-, and 12.5-km altitudes, black lines with arrows depicting sense of aircraft travel), and those segments of the legs (yellow highlighting) for which moderate-or-greater turbulence was diagnosed in the flight-level data. Also shown is the vertical cross section of wind magnitude (blue lines, 5 m s^{-1} isotachs), potential temperature (black lines, 2K isentropes), and DTF turbulence diagnostic computed from dropsondes (note release times at bottom of display) from 23:26:06 UTC 17 February through 00:24:02 UTC 18 February 2001. Jet core is highlighted by winds in excess of 80 m s^{-1} (maximum of 100 m s^{-1}), and DTF values are contoured at 0.6 and $1.0 \text{ m}^2 \text{ s}^{-3}$ (yellow and red areas, respectively). Note distance scale at top of display.

frequency selection and intermittency nature, and the time (or spatial) scales are related to those of geo-fluid turbulence (Fig. 2a and 2d), whereas the slow signals displayed strong signal selection, and can be retrieved as a packet of small-scale gravity waves (Fig. 2b-c; Lu et al 2005a). Koch et al (2005) showed that the upper-level jet streak (see Fig. 1) served as a source of unbalanced flow, which initiated a packet of mesoscale inertia-gravity waves (a few hundred kilometers in wavelength), and the small-scale gravity waves were generated through continuous scale cascade down from mesoscale inertia-gravity waves via wave-wave interaction.

Gravity-wave Polarization and Turbulence Generation

If the slow signals presented in Fig. 2 were identified as a packet of small-scale gravity waves, the horizontal velocity compo-

(continued on page 13)

Turbulence Generation *(continued from page 12)*

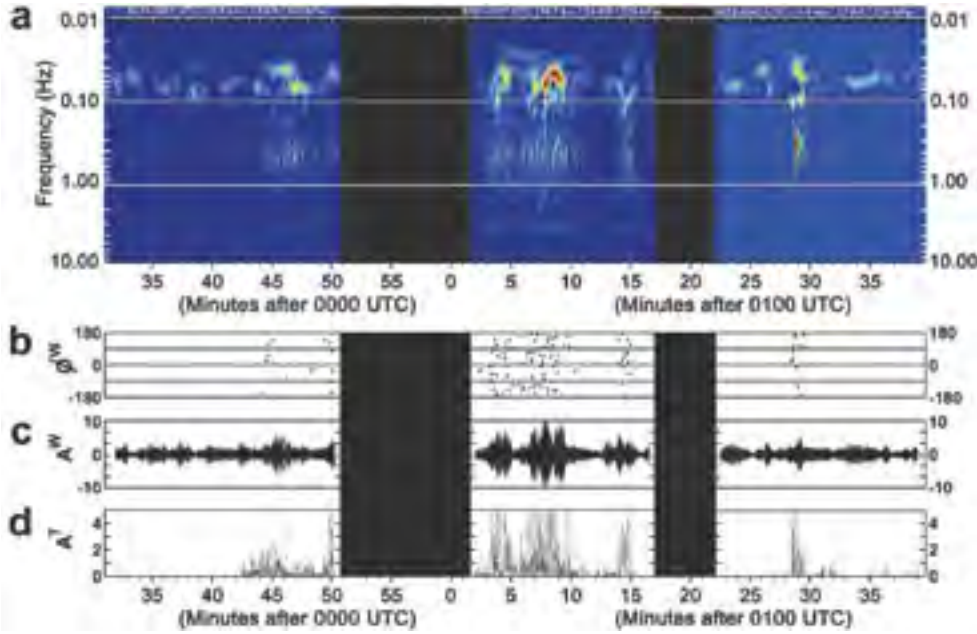


Figure 2: a) Time-frequency display of wavelet analysis of aircraft vertical acceleration data at 10.1, 10.7, and 11.4 km flight altitudes ($m s^{-2}$); b) Phase of gravity waves (degrees) at which maximum turbulence intensity occurred for turbulence $> 0.5 m^2 s^{-4}$; c) Gravity waves reconstructed from wavelet analysis in the 0.07 frequency band; and d) Turbulence intensity ($m^2 s^{-4}$) reconstructed from wavelet analysis in the 0.65 Hz frequency band. Background noise level of wavelet amplitudes is depicted by blue, with increasing intensity shown by yellow and red shading. Black segments indicate times when the aircraft was going through maneuvers (primarily changes in altitude) that invalidated the measurements.

nents and temperature associated with these waves must satisfy certain polarization relationships (Lu et al 2005a). These polarization properties can be lost or drastically different for turbulence (Lu et al 2005b). In Fig. 3, we computed and plotted two of the Stokes parameters (parameters that measure the different aspects of wave polarization), coherency and phase difference between the two components of the horizontal winds for G-IV flight track at 10.1-km level, as functions of

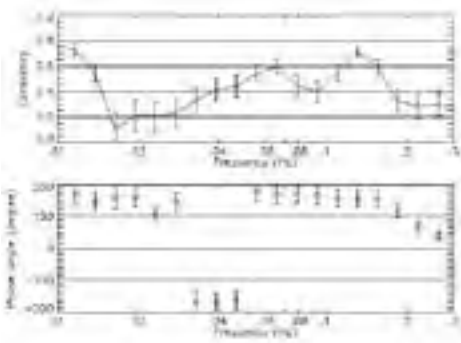


Figure 3: The coherency and phase-difference angle between two horizontal components of the wind as functions of frequency, computed from the set of Stokes parameters. The error bars indicate confidence intervals of the analyses (\pm twice the standard deviation of the time mean divided by the number of the sample size).

frequency ranging from 0.01 to 0.3 Hz. From the figures, one can see that there exists a distinctive spectral region, corresponding to small-scale gravity waves, which is consistent with the polarization theory (Lu et al 2005a). The degree of polarization is high (the coherency of u and v is > 0.6) for three waves (with frequencies of $\sim 0.01, 0.06,$ and 0.15 Hz). Corresponding to these three waves, the gravity-wave phase spectrum presents a clear polarization feature, since all phase-difference angles are clustered around $\pm 180^\circ$ for frequencies $f < 0.15$ Hz (Fig. 3b). At approximately 0.2 Hz, the coherency shows a significant drop, and the two horizontal wind components remain at a flat and low level of polarization. This is the same spectral region where the cross phase between u and v begins to fade away from their $\pm 180^\circ$ polarization. This transitional frequency from gravity waves to turbulence is consistent with that observed from Fig. 2.

Using the wavelet-based cross-spectral method, we could localize the above spectral results in the physical space to see how gravity wave polarization is related to the generation of turbulence. Figure 4a plots the turbulence intensity as a function of

time observed during the SCATCAT mission for flight track at 10.1-km level. For the same time domain, we plot the coherency and phase-difference angle for the averaged gravity-wave spectrum of the velocity data at that level. The shaded regions correspond to the time periods when significant turbulence occurrence was identified. One can see that the turbulence occurrence corresponds to times when gravity waves experience enhanced levels of polarization (Fig. 4b). However, there are more sharp peaks in the coherency time series when turbulence is identified. This indicates that in order for turbulence to occur, gravity waves need to have a higher level of polarization energy, and that the surge of turbulence is associated with an instantaneous energy leak from gravity waves to turbulence. When this happens, the polarization phase angle between u and v also tends to be altered (Fig. 4c) from their $\pm 180^\circ$ phase difference. These findings may have provided a basis for the forecast of turbulence, because the turbulence is on too small of a scale to be seen in any state-of-the-art atmospheric model (the turbulence is usually parameterized), whereas gravity waves can be simulated in quite some detail by high-resolution numerical prediction models.

Gravity Wave-turbulence Interaction, Kelvin-Helmholtz Instability, and Wave Breaking

The scale interaction between turbulence and gravity waves can be understood from the structure function analysis of observed wind and thermodynamic fields (Lu, et al 2005c). The structure function is computed by taking the difference of an observed variable at locations separated by distance r , then taking an ensemble average of this quantity with the same separation distance. The important features that come out of this computed quantity (the structure function), according to the Kolmogorov theory and the Oboukhov theory for isotropic turbulence, are the slope of the curve (the inertial range) and the sign of the values constituting the curve. The slope of the structure function depicts the scale of energy cascade for a particular physical process (scaling as $r^{2/3}$ for turbulence and r or higher order of r for gravity waves for the second-order structure function, and scaling

(continued on page 14)

Turbulence Generation *(continued from page 13)*

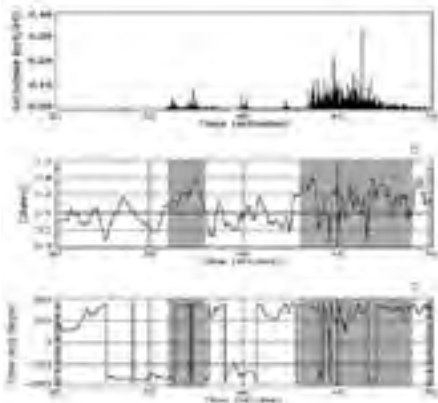


Figure 4: The localization of the turbulence intensity and the Stokes parameters in the time domain for the averaged gravity-wave spectrum ($f = 0.01-0.2$ Hz) using wavelet transformation: a) turbulence intensity; b) gravity-wave velocity coherency; and c) gravity-wave velocity phase-difference angle. The shaded regions indicate the time periods when turbulence is generated.

as r for turbulence and r^2 or r^3 for gravity waves for the third-order structure function) and the sign of the third-order structure function points in the direction of the energy cascade (positive for upscale and negative for down scale).

In Fig. 5, we plot the second-order structure functions at three different altitudes of 10.1-, 11.4-, and 12.5-km as functions of spatial distance r . As indicated in Fig. 1, gravity waves are present in all three of these flight levels, while turbulence is only observed at 10.1- and 11.4-km levels. It can be seen from Fig. 5 that at 12.5-km level where turbulence is not observed, the second-structure function (the thick-solid curve) follows, for the most part of spatial scale, the r scaling, and pushes the inertial scale to the very end of the scale range (to the dissipation range). The r scaling for the most part is the gravity-wave subrange. The very narrow range of $r^{2/3}$ at the tail of this curve is of course the turbulence inertial range scaling. At 10.1-km (dashed curve) and 11.4-km (dotted curve) levels, the presence of turbulence seems to have the effect of stretching the inertial range upscale, almost to the kilometer scale. Above approximately the 1-km scale, all levels' data displayed a gravity-wave scaling of r .

Figure 6 is a plot of the third-order structure functions for the observed horizontal velocity fields at 12.5-km level (solid curve), 11.4-km level (dotted curve), and 10.1-km level (dashed curve). Following convention,

we denote the red color for the negative sign in the calculated third-order structure function, representing the downscale energy cascade, and denote the blue color for the positive sign, representing the upscale energy cascade (inverse energy cascade). Several immediately identifiable features from this figure are: 1) extended inertial range with approximate r slope (verified with line-fitting of these curves) exists in the data of the two levels at 10.1 and 11.4 km where turbulence was observed; 2) the extended inertial range occupies spatial scales from a few tens of meters to a few hundred meters (close to the order of one kilometer); 3) for those data with observed turbulence, the gravity-wave subrange obeys an r^2 slope; 4) when there is no observed turbulence (at the 12.5-km level), the gravity wave obeys an r^3 slope; 5) the extended gravity-wave scaling at the 12.5-km level squashed the inertial range to the tail of the curve with relatively narrow spatial scales, ranging only to about 30 meters; and 6) no turbulence generation (at 12.5-km level) may be related to less energy input at the very large scale (relatively flat curves at the largest spatial scale ~ 100 km).

In addition to the above observations in Fig. 6, the most striking result is that at the 12.5-km level where no turbulence is generated, there seems to exist an “open” path for energy to cascade all the way through from large scale down to the dissipation scale (all red color), whereas when turbulence occurs at the 10.1-km and 11.4-km levels, there existed a very narrow scale (blue color), relative to which energy is converged from both large and small scales. For trained eyes, the only explanation for the presence of such inversed energy cascade scale and the whole physical process is that Kelvin-Helmholtz instability must have been present and such instability causes gravity-wave breaking so that the energy continues to cascade down through the turbulence inertial range and dissipate at the tail range. There is a set of physical reasoning to support this postulation. First, inverse energy cascade is usually associated with relatively large (comparing to 3D isotropic turbulence) quasi-two-dimensional structure. Kelvin-Helmholtz wave is a flow regime that belongs to this 2D structure. Second, Kelvin-Helmholtz billows usually occur at scales from a few hundred meters to a few kilometers. The blue-color regions in

the curves for the 10.1- and 11.4-km levels are certainly consistent with these scales. Third, Kelvin-Helmholtz instability is known to be most conducive to the generation of turbulence. The fact that the turbulence inertial range occurred right after (in scale) the energy inverse cascade, as contrast in the case of 12.5-km level where there is no inverse cascade corresponding to no turbulence generation until close to the dissipation range, suggests this point.

Concluding Remark

We have presented a theory of turbulence generation associated with gravity waves in the upper troposphere and lower stratosphere from the wavelet time-frequency analysis, the gravity wave polarization analysis, and the structure function analysis of aircraft observational data during the SCATCAT experiment. Our future research will be concentrated on the idealized simulation of the complete process of the dynamics of baroclinically unstable upper-level jet, gravity wave initiation associated with the upper-level jet, gravity wave steepening and energy cascade, and turbulence generation.

Acknowledgments: Thanks to Brian Jamison (CIRA), who provided the SCATCAT aircraft data, to Ning Wang (CIRA), who assisted with the wavelet analysis, to Steven Koch (NOAA), Ed Tollerud (NOAA), and Brian Jamison, who provided the dropsonde analysis (Fig. 1), and to all above people for the discussions and team work during this research.

References

- Koch, S. E., B. D. Jamison, C. Lu, T. L. Smith, E. I. Tollerud, C. Girz, N. Wang, T. P. Lane, M. A. Shapiro, D. D. Parrish, and O. R. Cooper, 2005: Turbulence and gravity waves within an upper-level front, accepted, *J. Atmos. Sci.*
- Lu, C., S. E. Koch, and N. Wang, 2005a: Determination of temporal and spatial characteristics of gravity waves using cross-spectral analysis and wavelet transformation. *J. Geophys. Res.*, 110, D01109, doi:10.1029/2004JD004906.
- Lu, C., S. E. Koch, and N. Wang, 2005b: Stokes parameter analysis of a packet of turbulence-generating gravity waves. In review, *J. Geophys. Res.*

Lu, C., and Co-authors, 2005c: Spectral and structure function analysis of upper-troposphere horizontal velocity fields. Part I: Interaction of
(continued on page 15)

Modeling Study *(continued from page 7)*

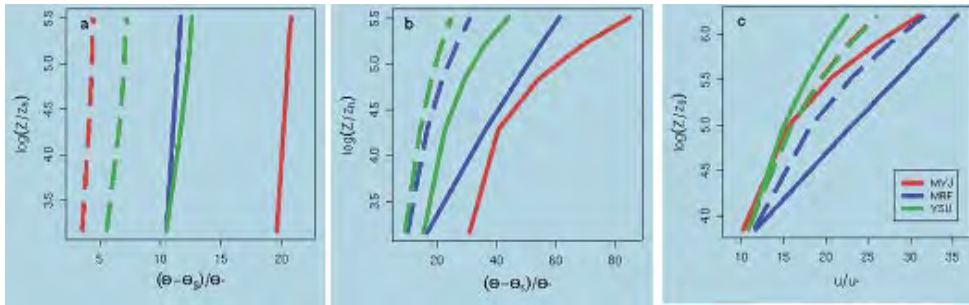


Figure 1: Profiles of potential temperature (a,b) and velocity (c) for the MYJ, MRF, and YSU schemes in the surface layer in convective (a) and stable (b,c) conditions. YSU overlays MRF in (a). YSU overlays MYJ in (b). Dashed lines denote profiles obtained using similarity.

also the case for the convective BL. The MRF fails to reproduce the curvature of the potential temperature profile, but instead generates a log-linear profile with insufficient mixing. The MYJ and YSU schemes quite accurately model momentum transfer while the MRF does not account for profile curvature in these conditions. In summary, behavior of the WRF in the SL when compared with similarity shows that all the

Method	Bias	RMSE	I of A	Correlation
Ave Ens	12.14	16.34	0.730	0.710
New Ens	0.16	10.08	0.843	0.708
Model A	5.16	16.80	0.698	0.464
Model B	3.50	11.90	0.796	0.648
Model C	5.61	13.18	0.769	0.630
Model D	17.81	25.13	0.617	0.620
Model E	10.81	16.22	0.685	0.572
Model F	27.81	33.10	0.502	0.569
Model G	14.51	22.56	0.647	0.630

Table 1: Bias, RMSE, index of agreement and correlation for the averaged ensemble and the weighted ensemble and for the individual models.

Turbulence Generation *(continued from page 14)*

turbulence and gravity waves, Kelvin-Helmholtz instability, and wave breaking. In the process to submit to *J. Geophys. Res.*

National Transportation Safety Board, 2003: Annual Review of Aircraft Accident Data, U.S. General Aviation, Calendar Year 1999. NTSB/ARG03-02.

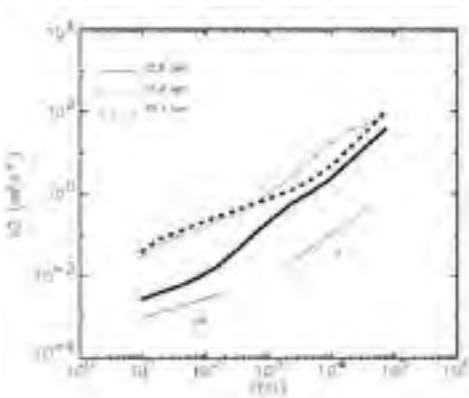


Figure 5: The second-order structure function as function of separation distance r in meters, for velocity data measured at 12.5-km level (solid curve), 11.4-km level (dotted curve), and 10.1-km level (dashed curve). The r and $r^{2/3}$ slopes are also drawn for reference.

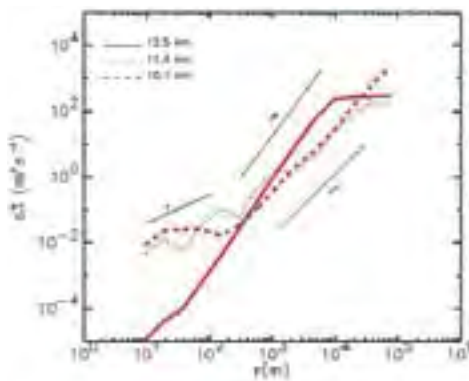


Figure 6: The third-order structure function as function of separation distance r in meters, for velocity data measured at 12.5-km level (solid curve), 11.4-km level (dotted curve), and 10.1-km level (dashed curve). The red color indicates that the computed values are negative, and the blue color indicates that the computed values are positive. The r , r^2 , and r^3 slopes are also drawn for reference.

schemes insufficiently transfer heat from/to the surface, suggesting that diurnal variation in the WRF SL, and consequently the entire BL, might be too weak or delayed, especially for the MYJ scheme. (Presented at the WRF Users' Workshop, Boulder, Colo., June 2004).

References

Hong, S.-Y, and J. Dudhia, 2003: Testing of a new non-local boundary layer vertical diffusion scheme in numerical weather prediction applications, 20th Conference on Weather Analysis and Forecasting/16th Conference on Numerical Weather Prediction, Seattle, WA.

Hong, S.-Y, and H.-L. Pan, 1996: Non-local boundary layer vertical diffusion in Medium-Range Forecast model, *Mon. Wea. Rev.*, **124**, 1215-1238.

Janjic, Z, 2001: Nonsingular implementation of the Mellor-Yamada level 2.5 scheme in the NCEP Meso model, NCEP office note #437.

A Simple Method to Improve Ensemble-Based Ozone Forecasts

Forecasts from seven air quality models and ozone data collected over the eastern USA and southern Canada during July and August 2004 were used in creating a simple method to improve ensemble-based forecasts of maximum daily 1-hr and 8-hr averaged ozone concentrations. The method minimizes least-square error of ensemble forecasts by assigning weights for its members. The real-time ozone forecasts from this ensemble of models were statistically evaluated against the ozone observations collected for the AIRNow database comprising more than 350 stations. Application of this method significantly improves overall statistics of the weighted ensemble (bias, RMSE, index of agreement and correlation) compared to the averaged ensemble or any individual ensemble member as shown in Table 1. If a sufficient number of observations is available, it is recommended that weights be calculated daily; if not, a longer training phase will still provide a positive benefit (submitted to *Geophysical Research Letters*).

CIRA Mission

The Mission of the Institute is to conduct research in the atmospheric sciences of mutual benefit to NOAA, the University, the State and the Nation. The Institute strives to provide a center for cooperation in specified research program areas by scientists, staff and students, and to enhance the training of atmospheric scientists. Special effort is directed toward the transition of research results into practical applications in the weather and climate areas. In addition, multidisciplinary research programs are emphasized, and all university and NOAA organizational elements are invited to participate in CIRA's atmospheric research programs.

The Institute's research is concentrated in several theme areas that include global and regional climate, local and mesoscale weather forecasting and evaluation, applied cloud physics, applications of satellite observations, air quality and visibility, and societal and economic impacts, along with cross-cutting research areas of numerical modeling and education, training and outreach. In addition to CIRA's relationship with NOAA, the National Park Service also has an ongoing cooperation in air quality and visibility research that involves scientists from numerous disciplines, and the Center for Geosciences/ Atmospheric Research based at CIRA is a long-term program sponsored by the Department of Defense.

Cooperative Institute for Research
in the Atmosphere
College of Engineering-Foothills Campus
Colorado State University Fort Collins, CO 80523-1375
(970) 491-8448

www.cira.colostate.edu

If you know of someone who would also like to receive the CIRA Newsletter, or if there are corrections to your address, please notify us.